Toward Rapid and Sensitive Detection of SARS-CoV-2 with Functionalized Magnetic Nanoparticles

Jing Zhong,* Enja Laureen Rösch, Thilo Viereck, Meinhard Schilling, and Frank Ludwig

Cite This: https://dx.doi.org/10.1021/acssensors.0c02160

Read Online

ACCESS | 📊 Metrics & More | 📖 Article Recommendations

ABSTRACT: The outbreak of the severe acute respiratory syndrome coronavirus 2 (SARS-CoV-2) threatens global medical systems and economies and rules our daily living life. Controlling the outbreak of SARS-CoV-2 has become one of the most important and urgent strategies throughout the whole world. As of October 2020, there have not yet been any medicines or therapies to be effective against SARS-CoV-2. Thus, rapid and sensitive diagnostics is the most important measures to control the outbreak of SARS-CoV-2. Homogeneous biosensing based on magnetic nanoparticles (MNPs) is one of the most promising approaches for rapid and highly sensitive detection of biomolecules. This paper proposes an approach for rapid and sensitive detection of SARS-CoV-2 with functionalized MNPs via the measurement of their magnetic response in an ac magnetic field. For proof of concept, mimic SARS-CoV-2 consisting of spike proteins and polystyrene beads are used for experiments. Experimental results demonstrate that the proposed approach allows the rapid detection of mimic SARS-CoV-2 with a limit of detection of 0.084 nM (5.9 fmole). The proposed approach has great potential for designing a low-cost and point-of-care device for rapid and sensitive diagnostics of SARS-CoV-2.
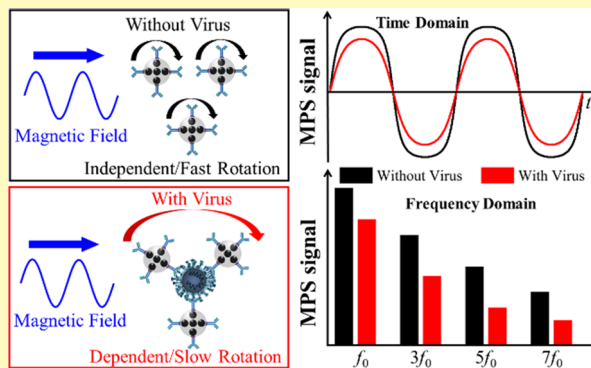
KEYWORDS: SARS-CoV-2, magnetic nanoparticles, ac susceptibility, magnetic particle spectroscopy, limit of detection

Severe acute respiratory syndrome coronavirus 2 (SARS-CoV-2) is an RNA-based virus that causes the coronavirus disease 2019 (COVID-19).[1] SARS-CoV-2 with a diameter ranging from about 60 to 140 nm has spike, envelope, membrane, and nucleocapsid proteins.[2,3] Spike protein is the one allowing the virus to bind to the receptor ACE2 of a host cell and to enter the host cell.[4,5] A patient infected with SARS-CoV-2 may suffer from severe pneumonia and acute respiratory distress syndrome.[3] Since the first infection case of SARS-CoV-2 reported in December 2019,[6,7] SARS-CoV-2 has spread across the whole world, which causes severe problems in medical systems, economics, and other social issues. Till early October 2020, World Health Organization (WHO) has reported more than 35 million cases of infection and 1 million deaths in the world. In addition to other control measures, e.g., social distancing and hand washing, WHO has strongly recommended a large amount of testing not only of symptomatic persons and their contacts but also of asymptomatic contacts. Therefore, large amounts of tests are one of the most important measures to control the outbreak of SARS-CoV-2. To date, polymerase chain reaction (PCR) based tests with high sensitivity and specificity are the gold standard for the diagnostics of SARS-CoV-2 infection.[8,9] PCR tests include several complex experimental procedures, which costs at least a few hours to get the test results. In a PCR test,

most experimental procedures require sophisticated and very expensive instrumentation and should be handled by experienced experts. Otherwise, there is a high chance for a false positive/negative result. It leads to huge efforts for medical staffs in the clinics, especially during the exponential increase in infection cases. In developing and underdeveloped countries, the situation for the diagnostics of SARS-CoV-2 with PCR is even worse due to the lack of equipped labs, instrumentation, and experienced experts. Therefore, it is of extreme importance and necessity to develop new methods and/or instrumentation for rapid diagnostics of SARS-CoV-2 with reasonable costs. WHO highly encourages researches on the performance of rapid diagnostics approaches. However, the development of new approaches for rapid diagnostics is still a challenging research topic.

In addition, there have been a variety of different approaches for the SARS-CoV-2 rapid diagnostic test based on the

detection of RNA, antibody, and antigen. For instance, the method of loop-mediated isothermal amplification (LAMP) was developed to realize nucleic acid amplification in a rather short time of about 30 min, which allows a limit of detection (LOD) of several tens of copies per mL.[10−12] However, it still requires professional staff to handle the experimental procedures with lab instruments. Alternatively, a plasmonic biosensor was reported to detect a SARS-CoV-2 RdRp gene through nucleic acid hybridization with an LOD of about 0.22 pM.[13] Antibody-based immunoassays for rapid diagnostics can only be applied to detect prior infections whereas antigen-based rapid tests allow the diagnosis of an on-going infection. The spike and nucleocapsid proteins of SARS-CoV-2 are the most promising biomarkers for antigen-based rapid diagnostics test. Seo et al. reported a graphene-based field-effect transistor biosensor to detect spike protein with an LOD of 1 fg/mL in phosphate-buffered saline (PBS) and 100 fg/mL in biological samples.[14] Although there have already been some approaches for point-of-care (POC) tests, rapid, inexpensive, and easy-to-use antigen-based immunoassay, are still highly demanded. A lateral flow assay (LFA) is one of the most promising approaches due to its low-cost, easy manufacture, full compatibility with POC test, and easy to use.[15] For instance, Baker et al. reported on a lateral flow POC diagnostic device to detect SARS-CoV-2 spike proteins with an LOD of about 5 μg/mL (5 nM) for under 30 min.[16] In principle, several approaches were reported to improve the sensitivity of LFAs with gold/silver nanoparticles (NPs).[17,18] Grant et al. developed an LFA for the detection of SARS-CoV-2 nucleocapsid proteins using an optical reader, which provided an LOD of about 0.65 ng/mL.[19] Several studies on different commercial antigen tests reported a wide range of sensitivities from 16.7 to 93.9%.[20−23] LFAs can only detect the antigen qualitatively or at most semi-quantitatively. For most of the promising rapid antigen-based tests that have been developed in research labs, it is still an open question about the performance for real applications. Therefore, there are still different approaches that are being investigated and/or tested for rapid, inexpensive, and easy-to-use antigen diagnostics.

Homogeneous biosensing based on magnetic nanoparticles (MNPs) is one of the most promising approaches for rapid and sensitive detection of analytes. The measurement of the dynamic magnetization of MNPs when exposed to time-varying magnetic fields is one way of homogeneous biosensing.[24] The binding behavior of the biomolecules to functionalized MNPs, dominated by Brownian relaxation, increases their hydrodynamic size or forms cross-linking structures, which significantly changes the Brownian relaxation time of the MNPs and their dynamic magnetization in time-varying magnetic fields.[25−27] For instance, in ac susceptibility (ACS) spectra, the peak frequency of the imaginary part of the MNPs bound with biomolecules shifts to lower frequencies due to the increase in effective hydrodynamic size.[28] In magnetic particle spectroscopy (MPS), the harmonics dominated by Brownian relaxation decrease when exposed to a sufficiently strong ac magnetic field. Especially, higher harmonics decrease faster than the fundamental harmonic, thus showing a decrease in the harmonic ratio.[25,29] Thus, the measurement of the MNP magnetization and its susceptibility/ spectra in ac magnetic fields can be used to detect the quantity of specific biomolecules. An MPS system has been demonstrated to be a low-cost, versatile, and sensitive tool to measure MNP magnetization and dynamics for biomolecule

detection.[25,30] For instance, MNP-based biosensing was developed via measuring the mixing-frequency components of the MNP dynamic magnetization in dual-frequency ac magnetic fields.[31−33] A mixing-frequency MPS system was designed to measure the mixing components of protein G-functionalized MNP magnetization for antibody detection.[34] Zhang et al. reported on the measurement of the harmonic ratio of anti-thrombin DNA aptamers-functionalized MNPs for the detection of thrombin.[35] Zhong et al. investigated the effect of binding behavior on the relaxation time of the streptavidin-coated MNPs and harmonic ratio for the detection and imaging of biotinylated IgG using streptavidin functionalized MNPs.[25] Yang et al. demonstrated the feasibility of wash-free, sensitive, and specific assays for the detection of different viruses, e.g., orchid and influenza viruses, with antibody-functionalized MNPs by measuring the reduction in the ACS in mixed-frequency ac magnetic fields.[36] In 2016, Tian et al. investigated the detection of Zika virus oligonucleotide via measuring the ACS of functionalized MNPs.[37] Wu et al. introduced a new biosensing scheme to detect H1N1 with functionalized MNPs. Here, the MPS signal of nucleoprotein molecule antibodies functionalized MNPs, especially the ratio of the 5th to 3rd harmonics was measured to quantify H1N1 nucleoprotein molecules.[38] In 2020, Tian et al. reported on homogeneous detection of SARS-CoV-2 utilizing an opto-magnetic measurement system for the detection of the RNA-dependent RNA polymerase coding sequence of SARS-CoV-2 with a sub-femtomolar LOD with a total assay time of about 100 min.[39] All these approaches have demonstrated that MNP-based homogeneous biosensing is a wash-free and a mix-and-measure approach for rapid and sensitive detection of specific biomolecules. Compared with the approaches based on gold/ silver NPs, e.g., LFAs, MNP-based homogeneous biosensing allows a quantitative detection of the analytes, as well as the measurements of reaction kinetics. Another key advantage is the possibility of the acceleration of the antigen−antibody reaction kinetics by the manipulation of the functionalized MNPs by external magnetic field gradients.[24] According to our knowledge, there have not yet been any approaches reporting on the detection of the SARS-CoV-2 antigen with MPS. Therefore, it is of great interest and importance to investigate MNP-based biosensing for rapid and sensitive detection of SARS-CoV-2.

In this paper, we propose the detection of SARS-CoV-2 by measuring the MPS signal of SARS-CoV-2 spike protein antibody-functionalized MNPs. For the proof of concept, SARS-CoV-2 spike protein antibody-functionalized MNPs are used as sensors to detect mimic SARS-CoV-2 that is a 100 nm polystyrene (PS) bead conjugated with SARS-CoV-2 spike proteins. A custom-built MPS system is used to measure the MPS signal of the functionalized MNPs. In addition, the ACS spectra are measured with a rotating magnetic field (RMF) system to evaluate the Brownian relaxation time. Experiments on samples with different mimic virus concentrations are performed to evaluate the measurement sensitivity and LOD of the present approach.

■ EXPERIMENTAL SECTION

Functionalized MNPs. In this paper, functionalized MNPs dominated by Brownian relaxation are used to detect a mimic SARS-CoV-2. The functionalized MNPs consist of BNF-80 NPs coated with protein A, purchased from micromod Partikeltechnologie GmbH (Rostock, Germany), and SARS-CoV-2 spike protein

monoclonal antibodies (anti-SARS-CoV-2 spike), purchased from Biomol GmbH (Hamburg, Germany), as shown in Figure 1a. The
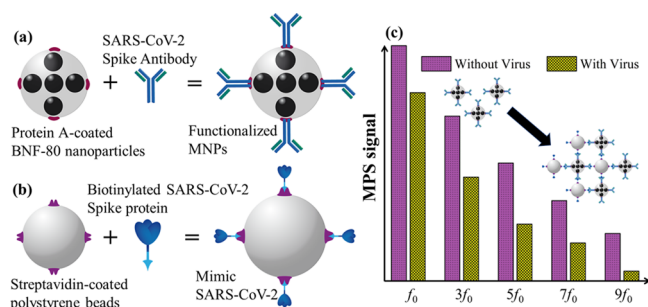

Figure 1. (a) Schematic of functionalized MNPs, (b) schematic of mimic SARS-CoV-2, and (c) schematic of the MPS signal with and without mimic virus.

protein A-coated BNF-80 NPs and SARS-CoV-2 spike protein antibodies are mixed and incubated at 4 °C for more than 12 h without any further washing steps. Due to the high binding affinity between protein A and the antibody Fc fragment, SARS-CoV-2 spike protein antibodies are easily conjugated onto the surface of protein A-coated BNF-80 NPs. BNF-80 NPs with protein A are multicore particles with a mean size of about 80 nm, which has an iron concentration of 5.5 mg/mL and a molar particle concentration of 20 pmole/mL (20 nM). The stock sample is diluted to 2 nM for experiments.

Mimic SARS-CoV-2. Each mimic SARS-CoV-2 consists of a single streptavidin-coated PS bead (purchased from micromod Partikeltechnologie GmbH) and 100 biotinylated SARS-CoV-2 spike proteins (RBD-SD1, Avi-His Tag, from Biomol GmbH), as shown in Figure 1b. The streptavidin-coated PS beads and the biotinylated SARS-CoV-2 spike proteins are mixed and incubated at 4 °C for more than 12 h without any further washing steps. Due to the high binding affinity between streptavidin and biotin, the biotinylated SARS-CoV-2 spike proteins are conjugated onto the surface of streptavidin-functionalized PS beads with a nominal size of 100 nm (similar to the size of SARS-CoV-2).[40]

Preparation of Experimental Samples. To make sure the conjugation between the antigen and antibody is finished, ACS spectra and MPS signal are measured in more than 1 h after mixing the functionalized MNPs and the mimic SARS-CoV-2. Totally, five experimental samples with different mimic virus concentrations from 0 to 3.38 nM are prepared. Note that, in this paper, all the mole quantity/concentration of mimic virus is given by that of PS beads. Each sample with a total volume of 90 μL consists of 0.18 pmole BNF-80 NPs and 4 pmole SARS-CoV-2 spike protein antibodies. For the functionalized MNPs, the quantity of the SARS-CoV-2 spike protein antibody is 4 pmole, which is according to preliminary tests, a balance between the binding affinity of the functionalized MNPs and an increase in their hydrodynamic sizes. For control experiments, the protein A-coated BNF-80 NPs without SARS-CoV-2 spike protein antibody are used to study the nonspecific binding between the unfunctionalized MNPs and the mimic SARS-CoV-2 as well as an increase in viscosity due to the presence of the mimic SARS-CoV-2.

Measurements. Exposed to a sufficiently strong ac magnetic field with excitation frequency f_0, the MPS signal consists of not only the fundamental harmonic at frequency f_0 but also higher harmonics M_i at frequency $i \times f_0$. Figure 1c shows the schematic of the MPS signal of the MNPs dominated by Brownian relaxation. In absence of mimic SARS-CoV-2, the functionalized MNPs can freely rotate, thus resulting in rich harmonic spectra. The present mimic SARS-CoV-2 binds to the functionalized MNPs, thus increasing the effective hydrodynamic size. Consequently, the functionalized MNPs cannot freely rotate or rotate slowly in response to the excitation magnetic field at the used frequency f_0, which significantly decreases the MPS signal. Therefore, the quantity of mimic SARS-CoV-2 can be

measured by the measurement of the MPS signal of the functionalized MNPs. In this paper, a detection coil-based scanning MPS system is used to measure the MPS signal in 10 mT-excitation magnetic field in the frequency range from 140 Hz to 1.4 kHz.[41] The measurement time amounts to about 9 s, including 1 s for sample measurement, 1 s for blank measurement, and 7 s for mechanical movement. In addition, a fluxgate sensor-based RMF system is used to measure the ACS spectra in a 0.5 mT-excitation magnetic field in the frequency range from 1 Hz to 3 kHz.[29] The sample volumes for the measurements of ACS spectra and MPS are 90 and 70 μL, respectively.

■ **RESULTS**

AC Susceptibility. Figure 2a,b shows the measured imaginary parts χ'' of the ACS spectra on the functionalized
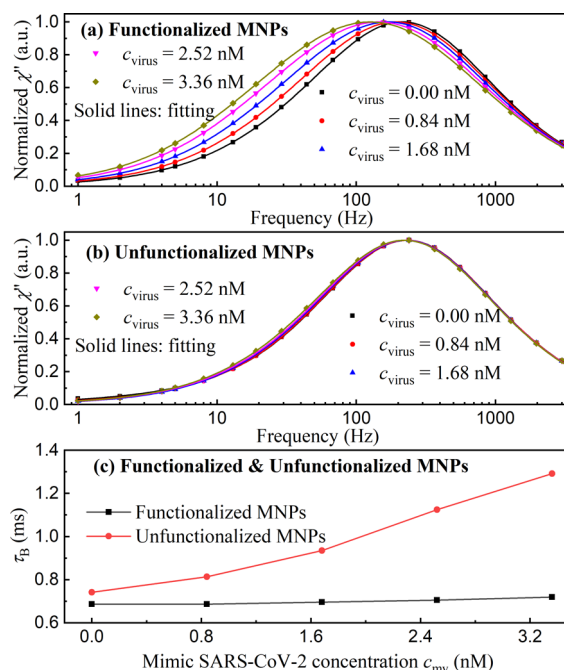

Figure 2. Experimental results of normalized imaginary parts χ'' of functionalized (a) and unfunctionalized (b) MNPs for different mimic virus concentrations. Symbols are experimental data, whereas solid lines are fits with a generalized Debye model. (c) Calculated effective Brownian relaxation time τ_B vs c_{mv} for functionalized and unfunctionalized MNPs. Symbols are experimental data, whereas solid lines are guides to the eyes.

and unfunctionalized MNPs, respectively. For functionalized MNPs, with increasing c_{mv}, the χ'' shape, shown in Figure 2a, gets broader while the peak frequency shifts to a lower frequency. This indicates an increase in the effective Brownian relaxation time τ_B.[25] For unfunctionalized MNPs, the χ'' shape, shown in Figure 2b, slightly shifts to lower frequencies with increasing c_{mv}. It may be caused by nonspecific binding between the mimic virus and the unfunctionalized MNPs, as well as an increase in the solution viscosity due to the presence of the mimic virus. The changes in χ'' of the functionalized MNPs are much more significant than those of the unfunctionalized MNPs, indicating that the specific binding behaviors between the SARS-CoV-2 antigen and antibody dominate.

To quantitatively investigate the dependence of the effective Brownian relaxation time τ_B on the mimic virus concentration c_{mv}, τ_B was estimated from the peak frequency of χ''. To

precisely determine the peak frequency despite the limited number of data points, χ'' were fitted with a generalized Debye model with a bimodal lognormal size distribution.[25] The solid lines in Figure 2a,b show that the generalized Debye model fits the experimental data very well. Then, τ_B was calculated via the peak frequency f_{peak} of the maximum in the fitted χ'' applying $\tau_B = 1/(2 \times \pi \times f_{peak})$. Figure 2c shows the dependence of τ_B on the c_{mv} of functionalized and unfunctionalized MNPs. For the unfunctionalized MNPs, τ_B increases by a factor of about 1.05 (from 0.687 to 0.719 ms), whereas for functionalized MNPs, τ_B significantly increases by a factor of about 1.74 (from 0.742 to 1.292 ms). Additional control experiments on ACS spectra were also performed with BNF-80 NPs functionalized with CD4 antibodies (not specific to SARS-CoV-2 spike protein) and the mimic virus (data not shown), which also show minor changes in τ_B. This indicates that the specific binding between SARS-CoV-2 antigen and antibody significantly increases τ_B. Note that, for $c_{mv} = 0$ nM, τ_B for the functionalized MNPs is greater than that for the unfunctionalized MNPs, which is caused by a larger hydrodynamic size of the functionalized MNPs due to the conjugation of SARS-CoV-2 spike protein antibodies onto the surface of the protein A-coated BNF-80 NPs. Therefore, our experimental results demonstrate that the specific binding of the mimic SARS-CoV-2 onto the surface of the functionalized MNPs significantly increases the effective Brownian relaxation time.

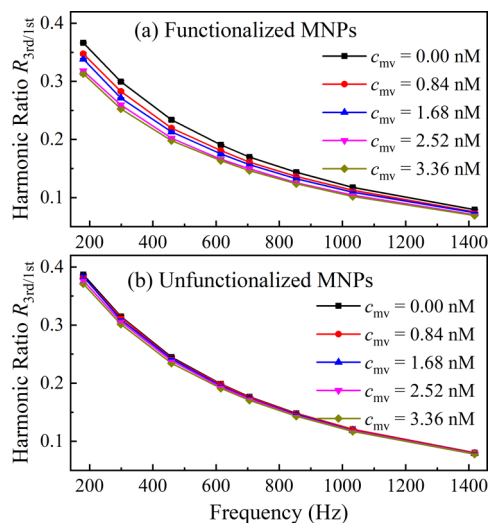**Magnetic Particle Spectroscopy.** Figure 3 shows the experimental results of the harmonic ratio $R_{3rd/1st} = M_3/M_1$ vs

Figure 3. Experimental results of measured harmonic ratio $R_{3rd/1st}$ vs excitation frequency of functionalized (a) and unfunctionalized (b) MNPs with different mimic virus concentrations c_{mv}, averaged by four independent repeat measurements. Symbols are experimental results, whereas solid lines are guides to the eyes.

frequency curves on samples with different c_{mv}. Note that the harmonic ratio is independent of the MNP concentration, but only dependent on c_{mv} in a given-frequency ac magnetic field. Figure 3a,b shows the experimental results of functionalized and unfunctionalized MNPs, respectively. The harmonic ratio $R_{3rd/1st}$ of the unfunctionalized MNPs slightly decreases with increasing c_{mv}, which might be caused by nonspecific binding and viscosity changes due to the presence of the mimic virus. On the other hand, the harmonic ratio $R_{3rd/1st}$ of the functionalized MNPs decreases significantly with an increase

in c_{mv}. Moreover, the changes in the $R_{3rd/1st}$ decrease with increasing excitation frequency, which agrees well with published results.[25] By comparing Figure 3a,b, the amounts of mimic SARS-CoV-2 can be quantified with $R_{3rd/1st}$ at each single excitation frequency. Note that Figure 3 also contains the error bars of the repeated measurements. Since the error bars (<0.002) are about 0.4% of the average $R_{3rd/1st}$, they are not discernable from Figure 3.

To quantitatively evaluate the changes in $R_{3rd/1st}$ vs c_{mv}, the change $\Delta R_{3rd/1st} = R_{3rd/1st}(c_{mv} = 0 \text{ nM}) - R_{3rd/1st}(c_{mv})$ was calculated and presented in Figure 4. Figure 4a,b shows

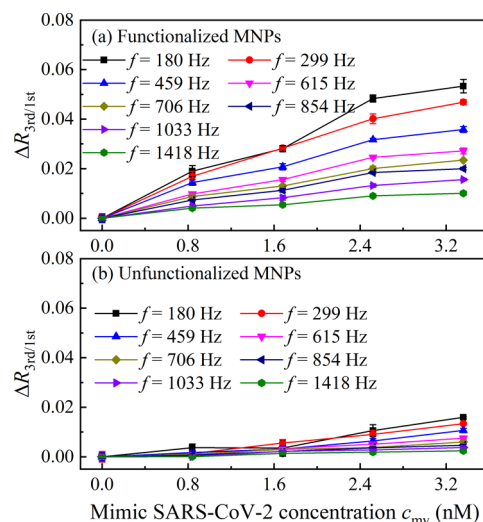**Figure 4.** Change in measured harmonic ratio $R_{3rd/1st}$ vs mimic SARS-CoV-2 concentration of functionalized (a) and unfunctionalized (b) MNPs at different excitation frequencies. Symbols are experimental results, whereas solid lines are guides to the eyes.

$\Delta R_{3rd/1st}$ vs c_{mv} curves of functionalized and unfunctionalized MNPs at different excitation frequencies, respectively. It clearly shows that the changes in $\Delta R_{3rd/1st}$ vs c_{mv} on the functionalized MNPs are much more significant than those on the unfunctionalized MNPs. With decreasing c_{mv}, the $\Delta R_{3rd/1st}$ values of the unfunctionalized MNPs decrease as well, indicating that the nonspecific binding or change in viscosity becomes less relevant at a low mimic virus concentration. The percentage of $\Delta R_{3rd/1st}$ for unfunctionalized MNPs to that for functionalized MNPs is less than 30%. In addition, it decreases to less than 20% with $c_{mv} = 0.84$ nM. Additional control experiments on the MPS signal were also performed with BNF-80 NPs functionalized with CD4 antibodies (not specific to SARS-CoV-2 spike protein) and the mimic virus (data not shown), which also show minor changes in $\Delta R_{3rd/1st}$. It means that the change in $\Delta R_{3rd/1st}$ is dominated by the specific binding between the antibody and antigen. Our experimental results demonstrate that the harmonic ratio $R_{3rd/1st}$ can be used for the detection of mimic SARS-CoV-2.

Limit of Detection. The LOD is one of the most important measures for sensitive detection. To evaluate the LOD, the measurement sensitivity S and noise level on the harmonic ratio are calculated. The measurement sensitivity, defined as the relative change in $\Delta R_{3rd/1st}$ to c_{mv} $d\Delta R_{3rd/1st}/dc_{mv}$, is calculated by a linear fitting of the $\Delta R_{3rd/1st}$ vs c_{mv} curves shown in Figure 4. Figure 5a shows the measurement sensitivity vs frequency curve. It indicates that with increasing frequency f_0 from 140 to 1418 Hz, the measurement sensitivity
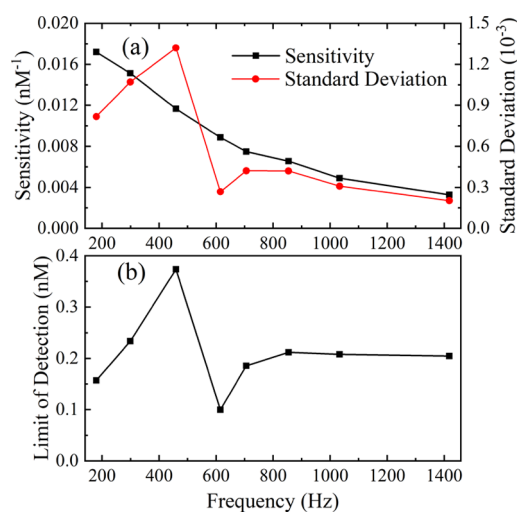
Figure 5. (a) Measurement sensitivity of mimic SARS-CoV-2 (left axis) and standard deviation (right axis) vs frequency curves. (b) Calculated limit of detection.

S decreases from 0.017 to 0.004 nM^{-1}, which quantitatively fits well with published results.[25] The noise level is calculated with the standard deviation σ of 10 repeated measurements on the harmonic ratio of an MNP sample with c_{mv} = 0 nM. In principle, with increasing f_0, the signal-to-noise ratio (SNR) of the measured harmonic gets improved, which would improve the standard deviation in a measured harmonic ratio due to Faraday's induction law. However, the data in frequencies of 299 and 459 Hz show higher noise levels than that in 180 Hz, which may be caused by instabilities of the measurement system. Figure 5b shows the LOD δ, estimated from the measurement sensitivity S and standard deviation σ by $\delta = 3.3$ σ/S.[42,43] Here, the factor of 3.3 corresponds for the 3 degrees of freedom (4 repeated measurements) to a confidence interval of about 95%. It indicates that the LOD is in the range from about 0.10 to 0.37 nM. Note that the estimated LOD is obtained for a single measurement.

To experimentally investigate the LOD of mimic SARS-CoV-2 with the present approach, several samples with low mimic virus concentrations are prepared. Figure 6 shows the $\Delta R_{3rd/1st}$ vs c_{mv} curves measured at different frequencies. The
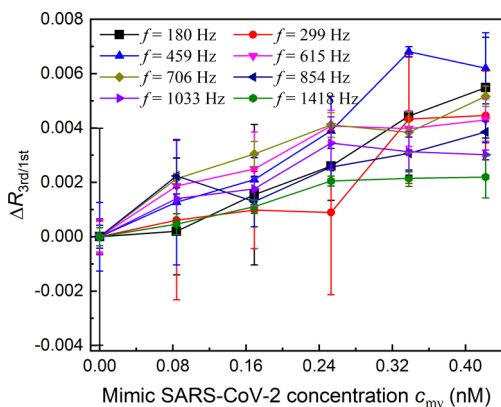

Figure 6. Experimental results of $\Delta R_{3rd/1st}$ vs mimic SARS-CoV-2 concentration at different frequencies. Experimental results are the average of four repeated measurements. Symbols are experimental data, whereas solid lines are guides to the eye.

experimental data were averaged from four repeated measurements with a total measurement time of about 36 s (note that each of the four cycles includes 1 s measurement on the MNP sample, 7 s mechanical movement of the robot, and 1 s background measurement). It clearly shows that for all the frequencies, the lowest mimic virus concentration of about 0.084 nM is detectable, which is slightly better than the estimated LOD from 0.05 to 0.18 nM with four repeated measurements. It might be caused by the underestimation of the measurement sensitivity since the measurement sensitivity is not obtained at very low concentrations of mimic virus. The present approach allows an LOD in terms of a mimic virus concentration of about 0.084 nM with a sample volume of about 70 μL and an LOD in terms of mole quantity of about 5.9 fmole.

■ DISCUSSION

Rapid and highly sensitive detection of SARS-CoV-2 is of great importance to control the outbreak of SARS-CoV-2, thus improving the pandemic situation. This paper proposed the detection of SARS-CoV-2 with functionalized MNPs via the measurements of the MPS signal, specifically the ratio of the 3rd to 1st harmonics. For a proof of concept, we used a 100 nm-size PS beads conjugated with SARS-CoV-2 spike protein to mimic SARS-CoV-2, while SARS-CoV-2 spike protein antibody-functionalized MNPs are used as sensors. Note that the functionalization of the MNPs via the binding affinity between protein A and antibody Fc fragment is not very stable, which may cause the bound antibody to elute from the MNPs in liquids with different pH values. For real applications, the SARS-CoV-2 spike protein antibody should be directly conjugated onto the surface of MNPs.[44] In this case, the functionalized MNPs can be stored for months, thus being deliverable and applicable to real biological samples. Our experimental results show that the present approach allows a highly sensitive detection of mimic SARS-CoV-2 with an LOD of about 0.084 nM (5.9 fmole) with four repeated measurements for about 36 s, including 4 s for measurement on an MNP sample, 28 s for mechanical movement, and 4 s for background measurement.

LOD and specificity are the most important parameters for diagnostic tests. The specificity of the current approach mainly depends on the specificity of the spike protein antibody binding to SARS-CoV-2 spike proteins. According to different approaches, this specificity can be very high.[14,19,23] It means that the current approach, in principle, allows a specificity as high as other approaches using SARS-CoV-2 spike protein antibodies. In this paper, the control experiments performed with unfunctionalized MNPs and CD4 antibodies-functionalized MNPs demonstrate that the changes in the harmonic ratio is mainly caused by the binding behavior between the antigen and antibody. Nevertheless, further experiments should be performed to identify the specificity of the current approach. The LOD directly affects the sensitivity of the diagnostic test. Different approaches have reported on different LODs ranging from 1 fg/mL to 5 μg/mL (5 nM).[14,16,19] In general, LFAs have a relatively poor LOD. However, due to its easy-to-use and inexpensiveness, LFAs for SARS-CoV-2 rapid antigen detection have gained a lot of interest. Furthermore, different methods with gold/silver NPs have already been developed to improve the LOD.[17,18] The LOD realized in the current approach is comparable to some of other reported approaches, e.g., the LOD reported in ref 20. According to

PCR tests, the virus load can be as high as 1.34×10^{11} copies/mL,[45] suggesting that the current approach might have relevant LOD for SARS-CoV-2 diagnostics with biological samples. However, so far, no reliable data on the quantity of living virus in a biological sample are available. Thus, it is still difficult to completely evaluate the efficiency of the current approach for real applications.

Note that the LOD realized in the current approach is not the limit of MNP-based homogeneous biosensing. Different methods can be applied to improve the LOD. For instance, in this paper, the used MPS system was built for two-dimensional imaging, but not a single pixel measurement. With a tailored MPS system, we believe that the LOD can be further improved without any significant costs. For instance, a tailored MPS system can measure 36 averages of the MPS signal within a total measurement time of 36 s if a blank measurement is performed in advance. In this case, the LOD can be improved by a factor of $\sqrt{n}$ for n repeated measurements. In the sample preparation, the functionalized MNPs and the mimic virus were not washed. Thus, there may be some unbound antibodies in the functionalized MNP suspension, as well as unbound antigens in the mimic virus suspension. These unbound antibodies and antigens, in principle, worsen the LOD since some mimic viruses may bind to the unbound antibodies but not to the functionalized MNPs. With direct conjugation of antibodies and further steps to wash out the unbound antibodies/antigens, the LOD is expected to be further improved. The hydrodynamic size of the functionalized MNPs plays a significant role in the measurement sensitivity and LOD. The MNPs with a small hydrodynamic size allow a larger relative change in their hydrodynamic size upon analyte binding, thus improving the measurement sensitivity and LOD. Thus, MNPs with smaller hydrodynamic size but still a strong contribution from Brownian relaxation will improve the LOD. In addition, in the experiments in this paper, the functionalized MNPs with a concentration of 20 nM were used. A smaller amount of MNPs will increase the measurement sensitivity according to the law of mass action discussed in our previous work, but worsen the SNR.[29,46] It means that there should be an optimum MNP concentration for biosensing in terms of LOD. In this case, a tailored MPS system with a high SNR will also improve the LOD since a lower amount of MNPs can be used. Several future works are planned to be done, including the design of a tailored MPS system to improve the SNR and the direct conjugation of spike protein antibodies onto the surface of MNPs, the study of different MNP systems and concentrations, and the diagnostics with real biological samples to evaluate the sensitivity and specificity.

WHO has developed the ASSURED criteria as a benchmark to evaluate if tests address disease control needs: affordable, sensitive, specific, user-friendly (simple to perform in a few steps with minimal training), rapid and robust (results available in less than 30 min), equipment-free, and deliverable to end users.[15,47] However, rare test methods can fit all the criteria in practice. MNP-based homogeneous biosensing only requires the mixture of the functionalized MNPs and the sample to be tested without any additional washing steps. The test results can be available in some seconds without taking into account the time required for antigen and antibody conjugation. Finally, the consuming time for the test results with the approach of MNP-based homogeneous biosensing mainly depends on the kinetic of SARS-CoV-2 antigen and antibody, which is in the order of about 10 min. Note that the current

approach does not require any complex sample preparation procedures, such as washing steps, but only sample collection, suspending samples from swab in a proper solution, and incubation of the sample and functionalized MNPs. It means that the present approach is sensitive, specific, and rapid and robust. The required materials, functionalized MNPs, are affordable, harmless, and deliverable to end users. Thus, it fits all the ASSURED criteria except equipment-free. However, the measurement setup, an MPS system, which consists of Helmholtz/solenoid coils for the generation of magnetic fields, pickup coils for the detection of MNP magnetization, some basic electronics for power amplifiers, preamplifiers and analog-to-digital/digital-to-analog converters, can be built as a point-of-care (POC) device with a low cost. For ultrasensitive detection of the analyte with the absolute signal from the magnetic response of functionalized MNPs, e.g., susceptibility and harmonic amplitude, the LOD may be dominated by the preparation error in the MNP concentration for measurements. The current approach employs the harmonic ratio of the 3rd to the 1st harmonics for biosensing, which is independent of the MNP concentration but only dependent on the analyte concentration, thus eliminating the preparation error in the MNP concentration. Therefore, we believe that the present approach is one of the most promising approaches for rapid diagnostic of SARS-CoV-2 in terms of the ASSURED criteria.

For SARS-CoV-2, there have been still a lot of open questions to be investigated. For instance, it is still an open question how many living viruses are in a biological sample and how high the infectious possibility is for asymptomatic infection cases. Approaches for RNA detection only give the information on the RNA concentration. It means that they can only diagnose whether a patient has been infected or not, but not provide the infection status. For instance, RNA-based test may not distinguish some infected patients with self-recovery who may just have some left virus RNAs but no living viruses. An approach of living virus detection will give some further information on the quantity of living viruses in a saliva sample, which is of great importance for medical doctors to evaluate the infectiousness. We believe that the present approach allows not only highly sensitive, rapid, and quantitative detection of living virus but also the evaluation of the infection status. The current approach can be used alone for SARS-CoV-2 diagnostics for decision making. In addition, combination of RNA and living virus detection will significantly contribute not only to SARS-CoV-2 diagnostics for decision but also to the understanding of the infection status and infectiousness. For the functionalized MNPs bound with 100 nm viruses, the change in the hydrodynamic size is much more significant than that for the functionalized MNPs bound with spike proteins. Thus, the direct detection of the virus, in principle, is more sensitive than that of the spike protein. Furthermore, the current approach employs the measurement of a magnetic signal of the functionalized MNPs, which does not have depth limitation. When combining with multicolor magnetic particle imaging,[48−50] the present approach can be extended to visualize the spatial distribution of SARS-CoV-2 in vivo, which is of great significance and interest not only to control the outbreak of SARS-CoV-2 but also to fundamental researches, e.g., understanding the underlying mechanisms of the infection process and virus proliferation.

CONCLUSIONS

This paper investigated rapid and sensitive detection of SARS-CoV-2 with functionalized MNPs. For a proof of concept, functionalized MNPs were used as sensors to detect a mimic virus consisting of 100 nm PS beads conjugated with SARS-CoV-2 spike proteins. Experiments on ACS spectra and MPS signal of samples with different mimic virus concentrations were performed. Experimental results showed that the binding behavior between mimic SARS-CoV-2 and functionalized MNPs increases the effective Brownian relaxation time and changing the MPS signal. The change in the ratio of the 3rd to 1st harmonics with the mimic virus concentration was used to analyze the measurement sensitivity and limit of detection. We believe that the current approach is of great promise to highly sensitive and rapid detection with a low cost, easy handling of the sample to be detected (mix-and-measure). The current approach is based on the quantitative measurements of the magnetic responses of functionalized MNPs, thus allowing the quantitative detection of SARS-CoV-2 virus particles. We envisage that the present work is of great interest and significance to develop new methods and design point-of-care devices for rapid diagnostics of SARS-CoV-2 to control its outbreak, as well as fundamental researches on the virus infection.

AUTHOR INFORMATION

Corresponding Author

Jing Zhong − Institute for Electrical Measurement Science and Fundamental Electrical Engineering and Laboratory for Emerging Nanometrology (LENA), TU Braunschweig, Braunschweig D-38106, Germany; orcid.org/0000-0002-8815-4105; Email: j.zhong@tu-braunschweig.de

Authors

Enja Laureen Rösch − Institute for Electrical Measurement Science and Fundamental Electrical Engineering and Laboratory for Emerging Nanometrology (LENA), TU Braunschweig, Braunschweig D-38106, Germany

Thilo Viereck − Institute for Electrical Measurement Science and Fundamental Electrical Engineering and Laboratory for Emerging Nanometrology (LENA), TU Braunschweig, Braunschweig D-38106, Germany

Meinhard Schilling − Institute for Electrical Measurement Science and Fundamental Electrical Engineering and Laboratory for Emerging Nanometrology (LENA), TU Braunschweig, Braunschweig D-38106, Germany

Frank Ludwig − Institute for Electrical Measurement Science and Fundamental Electrical Engineering and Laboratory for Emerging Nanometrology (LENA), TU Braunschweig, Braunschweig D-38106, Germany; orcid.org/0000-0002-2476-1352

Complete contact information is available at:
https://pubs.acs.org/10.1021/acssensors.0c02160

Author Contributions

All authors have given approval to the final version of the manuscript.

Notes

The authors declare no competing financial interest.

REFERENCES

(1) Gorbalenya, A. E.; Baker, S. C.; Baric, R. S.; de Groot, R. J.; Drosten, C.; Gulyaeva, A. A.; Haagmans, B. L.; Lauber, C.; Leontovich, A. M.; Neuman, B. W.; Penzar, D.; Perlman, S.; Poon, L. L. M.; Samborskiy, D. V.; Sidorov, I. A.; Sola, I.; Ziebuhr, J.; Coronaviridae Study Group of the International Committee on Taxonomy of Viruses. The Species Severe Acute Respiratory Syndrome-Related Coronavirus: Classifying 2019-NCoV and Naming It SARS-CoV-2. Nat. Microbiol. 2020, 5, 536−544.

(2) Kumar, S.; Nyodu, R.; Maurya, V. K.; Saxena, S. K. Morphology, Genome Organization, Replication, and Pathogenesis of Severe Acute Respiratory Syndrome Coronavirus 2 (SARS-CoV-2). Springer 2020, 23−31.

(3) Zhu, N.; Zhang, D.; Wang, W.; Li, X.; Yang, B.; Song, J.; Zhao, X.; Huang, B.; Shi, W.; Lu, R.; Niu, P.; Zhan, F.; Ma, X.; Wang, D.; Xu, W.; Wu, G.; Gao, G. F.; Tan, W.; China Novel Coronavirus Investigating and Research Team. A Novel Coronavirus from Patients with Pneumonia in China, 2019. N. Engl. J. Med. 2020, 382, 727−733.

(4) Wrapp, D.; Wang, N.; Corbett, K. S.; Goldsmith, J. A.; Hsieh, C. L.; Abiona, O.; Graham, B. S.; McLellan, J. S. Cryo-EM Structure of the 2019-NCoV Spike in the Prefusion Conformation. Science 2020, 367, 1260−1263.

(5) Wang, Q.; Zhang, Y.; Wu, L.; Niu, S.; Song, C.; Zhang, Z.; Lu, G.; Qiao, C.; Hu, Y.; Yuen, K. Y.; Wang, Q.; Zhou, H.; Yan, J.; Qi, J. Structural and Functional Basis of SARS-CoV-2 Entry by Using Human ACE2. Cell 2020, 181, 894−904.e9.

(6) Lu, H.; Stratton, C. W.; Tang, Y. W. Outbreak of Pneumonia of Unknown Etiology in Wuhan, China: The Mystery and the Miracle. J. Med. Virol. 2020, 401−402.

(7) Wu, F.; Zhao, S.; Yu, B.; Chen, Y. M.; Wang, W.; Song, Z. G.; Hu, Y.; Tao, Z. W.; Tian, J. H.; Pei, Y. Y.; Yuan, M. L.; Zhang, Y. L.; Dai, F. H.; Liu, Y.; Wang, Q. M.; Zheng, J. J.; Xu, L.; Holmes, E. C.; Zhang, Y. Z. A New Coronavirus Associated with Human Respiratory Disease in China. Nature 2020, 265−269.

(8) Long, C.; Xu, H.; Shen, Q.; Zhang, X.; Fan, B.; Wang, C.; Zeng, B.; Li, Z.; Li, X.; Li, H. Diagnosis of the Coronavirus Disease (COVID-19): RRT-PCR or CT? Eur. J. Radiol. 2020, 108961.

(9) Corman, V. M.; Landt, O.; Kaiser, M.; Molenkamp, R.; Meijer, A.; Chu, D. K. W.; Bleicker, T.; Brünink, S.; Schneider, J.; Schmidt, M. L.; Mulders, D. G. J. C.; Haagmans, B. L.; Van Der Veer, B.; Van Den Brink, S.; Wijsman, L.; Goderski, G.; Romette, J. L.; Ellis, J.; Zambon, M.; Peiris, M.; Goossens, H.; Reusken, C.; Koopmans, M. P. G.; Drosten, C. Detection of 2019 Novel Coronavirus (2019-NCoV) by Real-Time RT-PCR. Eurosurveillance. 2020, DOI: 10.2807/1560-7917.ES.2020.25.3.2000045.

(10) Yu, L.; Wu, S.; Hao, X.; Dong, X.; Mao, L.; Pelechano, V.; Chen, W.-H.; Yin, X. Rapid Detection of COVID-19 Coronavirus Using a Reverse Transcriptional Loop-Mediated Isothermal Amplification (RT-LAMP) Diagnostic Platform. Clin. Chem. 2020, 66, 975−977.

(11) Udugama, B.; Kadhiresan, P.; Kozlowski, H. N.; Malekjahani, A.; Osborne, M.; Li, V. Y. C.; Chen, H.; Mubareka, S.; Gubbay, J. B.; Chan, W. C. W. Diagnosing COVID-19: The Disease and Tools for Detection. ACS Nano 2020, 14, 3822−3835.

(12) Cui, F.; Zhou, H. S. Diagnostic Methods and Potential Portable Biosensors for Coronavirus Disease 2019. Biosens. Bioelectron. 2020, 165, 112349.

(13) Qiu, G.; Gai, Z.; Tao, Y.; Schmitt, J.; Kullak-Ublick, G. A.; Wang, J. Dual-Functional Plasmonic Photothermal Biosensors for Highly Accurate Severe Acute Respiratory Syndrome Coronavirus 2 Detection. *ACS Nano* **2020**, *14*, 5268−5277.

(14) Seo, G.; Lee, G.; Kim, M. J.; Baek, S.-H.; Choi, M.; Ku, K. B.; Lee, C.-S.; Jun, S.; Park, D.; Kim, H. G.; Kim, S.-J.; Lee, J.-O.; Kim, B. T.; Park, E. C.; Kim, S. I. Rapid Detection of COVID-19 Causative Virus (SARS-CoV-2) in Human Nasopharyngeal Swab Specimens Using Field-Effect Transistor-Based Biosensor. *ACS Nano* **2020**, *14*, 5135−5142.

(15) Pokhrel, P.; Hu, C.; Mao, H. Detecting the Coronavirus (CoVID-19). *ACS Sens.* **2020**, *5*, 2283−2296.

(16) Baker, A. N.; Richards, S.-J.; Guy, C. S.; Congdon, T. R.; Hasan, M.; Zwetsloot, A. J.; Gallo, A.; Lewandowski, J. R.; Stansfeld, P. J.; Straube, A.; Walker, M.; Chessa, S.; Pergolizzi, G.; Dedola, S.; Field, R. A.; Gibson, M. I. The SARS-COV-2 Spike Protein Binds Sialic Acids and Enables Rapid Detection in a Lateral Flow Point of Care Diagnostic Device. *ACS Cent. Sci.* **2020**, *6*, 2046−2052.

(17) Liou, P.; Nayigiziki, F. X.; Kong, F.; Mustapha, A.; Lin, M. Cellulose Nanofibers Coated with Silver Nanoparticles as a SERS Platform for Detection of Pesticides in Apples. *Carbohydr. Polym.* **2017**, *157*, 643−650.

(18) Yew, C.-H. T.; Azari, P.; Choi, J. R.; Li, F.; Pingguan-Murphy, B. Electrospin-Coating of Nitrocellulose Membrane Enhances Sensitivity in Nucleic Acid-Based Lateral Flow Assay. *Anal. Chim. Acta* **2018**, *1009*, 81−88.

(19) Grant, B. D.; Anderson, C. E.; Williford, J. R.; Alonzo, L. F.; Glukhova, V. A.; Boyle, D. S.; Weigl, B. H.; Nichols, K. P. SARS-CoV-2 Coronavirus Nucleocapsid Antigen-Detecting Half-Strip Lateral Flow Assay Toward the Development of Point of Care Tests Using Commercially Available Reagents. *Anal. Chem.* **2020**, *92*, 11305−11309.

(20) Weitzel, T.; Legarraga, P.; Iruretagoyena, M.; Pizarro, G.; Vollrath, V.; Araos, R.; Munita, J. M.; Porte, L. *Head-to-Head Comparison of Four Antigen-Based Rapid Detection Tests for the Diagnosis of SARS-CoV-2 in Respiratory Samples.* bioRxiv 2020, DOI: 10.1101/2020.05.27.119255.

(21) Lambert-Niclot, S.; Cuffel, A.; Le Pape, S.; Vauloup-Fellous, C.; Morand-Joubert, L.; Roque-Afonso, A.-M.; Le Goff, J.; Delaugerre, C. Evaluation of a Rapid Diagnostic Assay for Detection of SARS CoV-2 Antigen in Nasopharyngeal Swab. *J. Clin. Microbiol.* **2020**, *58*, e00977.

(22) Scohy, A.; Anantharajah, A.; Bodéus, M.; Kabamba-Mukadi, B.; Verroken, A.; Rodriguez-Villalobos, H. Low Performance of Rapid Antigen Detection Test as Frontline Testing for COVID-19 Diagnosis. *J. Clin. Virol.* **2020**, *129*, 104455.

(23) Porte, L.; Legarraga, P.; Vollrath, V.; Aguilera, X.; Munita, J. M.; Araos, R.; Pizarro, G.; Vial, P.; Iruretagoyena, M.; Dittrich, S.; Weitzel, T. Evaluation of Novel Antigen-Based Rapid Detection Test for the Diagnosis of SARS-CoV-2 in Respiratory Samples. *Int. J. Infect. Dis.* **2020**, *99*, 328−333.

(24) Schrittwieser, S.; Pelaz, B.; Parak, W. J.; Lentijo-Mozo, S.; Soulantica, K.; Dieckhoff, J.; Ludwig, F.; Guenther, A.; Tschöpe, A.; Schotter, J. Homogeneous Biosensing Based on Magnetic Particle Labels. *Sensors* **2016**, *16*, 828.

(25) Zhong, J.; Schilling, M.; Ludwig, F. Magnetic Nanoparticle-Based Biomolecule Imaging with a Scanning Magnetic Particle Spectrometer. *Nanotechnology* **2020**, *31*, 225101.

(26) Heim, E.; Ludwig, F.; Schilling, M. Binding Assays with Streptavidin-Functionalized Superparamagnetic Nanoparticles and Biotinylated Analytes Using Fluxgate Magnetorelaxometry. *J. Magn. Magn. Mater.* **2009**, *321*, 1628−1631.

(27) Hong, C. Y.; Wu, C. C.; Chiu, Y. C.; Yang, S. Y.; Horng, H. E.; Yang, H. C. Magnetic Susceptibility Reduction Method for Magnetically Labeled Immunoassay. *Appl. Phys. Lett.* **2006**, *88*, 212512.

(28) Astalan, A. P.; Ahrentorp, F.; Johansson, C.; Larsson, K.; Krozer, A. Biomolecular Reactions Studied Using Changes in Brownian Rotation Dynamics of Magnetic Particles. *Biosens. Bioelectron.* **2004**, *19*, 945−951.

(29) Zhong, J.; Janssen, K. J.; Draack, S.; Viereck, T.; Schilling, M.; Ludwig, F. Dependence of Biomolecule Detection on Magnetic Nanoparticle Concentration. *J. Magn. Magn. Mater.* **2021**, *517*, 167408.

(30) Wu, K.; Liu, J.; Su, D.; Saha, R.; Wang, J. P. Magnetic Nanoparticle Relaxation Dynamics-Based Magnetic Particle Spectroscopy (MPS) for Rapid and Wash-Free Molecular Sensing. *ACS Appl. Mater. Interfaces* **2019**, *11*, 22979−22986.

(31) Krause, H.-J.; Wolters, N.; Zhang, Y.; Offenhäusser, A.; Miethe, P.; Meyer, M. H. F.; Hartmann, M.; Keusgen, M. Magnetic Particle Detection by Frequency Mixing for Immunoassay Applications. *J. Magn. Magn. Mater.* **2007**, *311*, 436−444.

(32) Nikitin, P. I.; Vetoshko, P. M.; Ksenevich, T. I. New Type of Biosensor Based on Magnetic Nanoparticle Detection. *J. Magn. Magn. Mater.* **2007**, *311*, 445−449.

(33) Orlov, A. V.; Bragina, V. A.; Nikitin, M. P.; Nikitin, P. I. Rapid Dry-Reagent Immunomagnetic Biosensing Platform Based on Volumetric Detection of Nanoparticles on 3D Structures. *Biosens. Bioelectron.* **2016**, *79*, 423−429.

(34) Tu, L.; Jing, Y.; Li, Y.; Wang, J. P. Real-Time Measurement of Brownian Relaxation of Magnetic Nanoparticles by a Mixing-Frequency Method. *Appl. Phys. Lett.* **2011**, *98*, 213702.

(35) Zhang, X.; Reeves, D. B.; Perreard, I. M.; Kett, W. C.; Griswold, K. E.; Gimi, B.; Weaver, J. B. Molecular Sensing with Magnetic Nanoparticles Using Magnetic Spectroscopy of Nanoparticle Brownian Motion. *Biosens. Bioelectron.* **2013**, 441−446.

(36) Yang, S. Y.; Chieh, J. J.; Wang, W. C.; Yu, C. Y.; Lan, C. B.; Chen, J. H.; Horng, H. E.; Hong, C. Y.; Yang, H. C.; Huang, W. Ultra-Highly Sensitive and Wash-Free Bio-Detection of H5N1 Virus by Immunomagnetic Reduction Assays. *J. Virol. Methods* **2008**, 250−252.

(37) Tian, B.; Qiu, Z.; Ma, J.; de la Torre, T. Z. G.; Johansson, C.; Svedlindh, P.; Strömberg, M. Attomolar Zika Virus Oligonucleotide Detection Based on Loop-Mediated Isothermal Amplification and AC Susceptometry. *Biosens. Bioelectron.* **2016**, *86*, 420−425.

(38) Wu, K.; Liu, J.; Saha, R.; Su, D.; Krishna, V. D.; Cheeran, M. C.-J.; Wang, J.-P. Magnetic Particle Spectroscopy for Detection of Influenza A Virus Subtype H1N1. *ACS Appl. Mater. Interfaces* **2020**, *12*, 13686−13697.

(39) Tian, B.; Gao, F.; Fock, J.; Dufva, M.; Hansen, M. F. Homogeneous Circle-to-Circle Amplification for Real-Time Opto-magnetic Detection of SARS-CoV-2 RdRp Coding Sequence. *Biosens. Bioelectron.* **2020**, *165*, 112356.

(40) Bar-On, Y. M.; Flamholz, A.; Phillips, R.; Milo, R. Science Forum: SARS-CoV-2 (COVID-19) by the Numbers. *Elife* **2020**, *9*, e57309.

(41) Zhong, J.; Schilling, M.; Ludwig, F. Magnetic Nanoparticle Temperature Imaging with a Scanning Magnetic Particle Spectrometer. *Meas. Sci. Technol.* **2018**, *29*, 115903.

(42) Shrivastava, A.; Gupta, V. Methods for the Determination of Limit of Detection and Limit of Quantitation of the Analytical Methods. *Chronicles of Young Scientists.* **2011**, *2*, 21−25.

(43) Thompson, M.; Ellison, S. L. R.; Wood, R. Harmonized Guidelines for Single-Laboratory Validation of Methods of Analysis (IUPAC Technical Report). *Pure Appl. Chem.* **2002**, *74*, 835−855.

(44) Grüttner, C.; Müller, K.; Teller, J.; Westphal, F.; Foreman, A.; Ivkov, R. Synthesis and Antibody Conjugation of Magnetic Nanoparticles with Improved Specific Power Absorption Rates for Alternating Magnetic Field Cancer Therapy. *J. Magn. Magn. Mater.* **2007**, *311*, 181−186.

(45) Pan, Y.; Zhang, D.; Yang, P.; Poon, L. L. M.; Wang, Q. Viral Load of SARS-CoV-2 in Clinical Samples. *Lancet Infect. Dis.* **2020**, *20*, 411−412.

(46) Yang, C. C.; Yang, S.-Y.; Chen, H. H.; Weng, W. L.; Horng, H.-E.; Chieh, J.-J.; Hong, C. Y.; Yang, H.-C. Effect of Molecule-Particle Binding on the Reduction in the Mixed-Frequency Alternating Current Magnetic Susceptibility of Magnetic Bio-Reagents. *J. Appl. Phys.* **2012**, *112*, 024704.

(47) Peeling, R. W.; Holmes, K. K.; Mabey, D.; Ronald, A. Rapid Tests for Sexually Transmitted Infections (STIs): The Way Forward. *Sexually Transmitted Infections.* **2006**, v1.

(48) Gleich, B.; Weizenecker, J. Tomographic Imaging Using the Nonlinear Response of Magnetic Particles. *Nature* **2005**, *435*, 1214−1217.

(49) Rahmer, J.; Halkola, A.; Gleich, B.; Schmale, I.; Borgert, J. First Experimental Evidence of the Feasibility of Multi-Color Magnetic Particle Imaging. *Physics in Medicine and Biology.* **2015**, *60*, 1775−1791.

(50) Viereck, T.; Kuhlmann, C.; Draack, S.; Schilling, M.; Ludwig, F. Dual-Frequency Magnetic Particle Imaging of the Brownian Particle Contribution. *J. Magn. Magn. Mater.* **2017**, *427*, 156−161.